CHEMISTRY OF MATERIALS

ARTICLE

pubs.acs.org/cm

Ambient Synthesis of $Au_{144}(SR)_{60}$ Nanoclusters in Methanol

Huifeng Qian and Rongchao Jin*

Department of Chemistry, Carnegie Mellon University, Pittsburgh, Pennsylvania 15213, United States

Supporting Information

ABSTRACT: We report a facile, one-pot method for synthesizing atomically monodisperse $Au_{144}(SR)_{60}$ nanoclusters under ambient conditions. In this method, gold salt precursor is first mixed with excess thiol and tetraoctylammonium bromide (TOABr) in methanol to form Au(I)-SR polymers. Then, Au(I)-SR is reduced by excess $NaBH_4$ (aqueous solution) to form nanoclusters. Interestingly, the initially formed, polydisperse Au nanoparticles are size-focused into two monodisperse gold nanoclusters: $Au_{144}(SR)_{60}$ (major product) and $Au_{25}(SR)_{18}$ (side product) over a ~5 h period. The side product ($Au_{25}(SR)_{18}$) can be easily removed by washing the product with acetone, giving rise to pure $Au_{144}(SR)_{60}$. This method is applicable to a number of thiol ligands, including PhC_2H_4SH and various $C_nH_{2n+1}SH$ (where $n = 4-8$). Some critical parameters to obtain pure $Au_{144}(SR)_{60}$ have been identified, including the methanol solvent (as opposed to toluene traditionally used), large thiol-to-Au ratios (≥ 4), the presence of O_2 and tetraoctylammonium halide (TOAX, where X = Br, Cl). The facile synthetic method and the product made by this method should largely contribute to the practical application of this new type of nanomaterial.

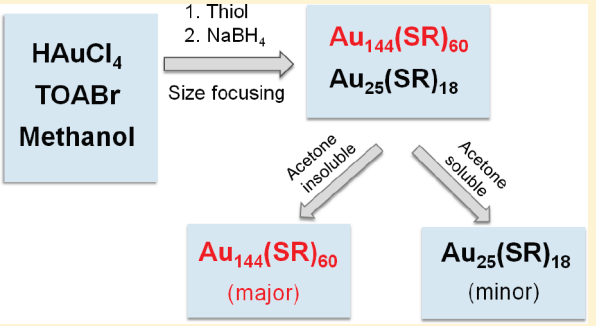

KEYWORDS: gold, nanoclusters, $Au_{144}(SR)_{60}$, atomic precision

INTRODUCTION

Thiolate-protected gold nanoparticles have found important applications in various fields, such as biology,[1−3] catalysis,[4−8] and sensors.[9] There are two interesting size regimes between the atomic state and the bulk metallic state, i.e., semiconducting nanoclusters and metallic nanocrystals.[10−12] When the size of gold nanoparticles is larger than ~2 nm, the particles adopt a face-centered cubic (fcc) structure and are in the metallic state. The optical properties of Au nanocrystals are dominated by surface plasmon resonance. On the other hand, when the particle size becomes less than ~2 nm, distinct effects of electron energy quantization occurs.[11,13−16] Interestingly, these ultrasmall nanoparticles (often called nanoclusters or clusters for short) do not adopt the fcc structure as in their larger counterparts—metallic Au nanocrystals. Because of quantum confinement effects, nanoclusters exhibit multiple, step-like absorption peaks in their optical spectra. The electrochemical experiments also indicate that these nanoclusters have a size-dependent energy gap.[10] In recent years, great advances have been attained in the synthesis, characterization and applications of metal nanoclusters.[16−31] Significant breakthroughs in this field are the X-ray crystal structure determination of $Au_{102}(SR)_{44}$, $Au_{25}(SR)_{18}^{0/-1}$ and $Au_{38}(SR)_{24}$ nanoclusters.[32−36] The structural information is critical for theoretical modeling and explaining the optical properties, stability, and magnetism of specific size Au nanoclusters.[34,37−40] The discovery of $Au(SR)_2$ and $Au_2(SR)_3$ "staple" motifs in the crystal structures is also important to understand the nature of thiol-gold surface bonding.[41]

Among the different sized nanoclusters, $Au_{144}(SR)_{60}$ has an important role in the study of gold nanoclusters. It lies in between smaller clusters (e.g., $Au_{25}(SR)_{18}$) that exhibit a distinct HOMO−LUMO gap and larger fcc crystalline Au nanoparticles that exhibit distinct surface plasmons.[42] In 1996, Whetten et al. first isolated a gold cluster species of 28−29 kDa core mass via solvent fractionation and identified the core to be approximately $Au_{\sim 140}$ by laser desorption ionization (LDI) mass spectrometry.[43] Murray and Quinn et al. found that the $Au_{\sim 140}$ nanoclusters showed intriguing quantized double layer charging in solution.[44−46] This cluster exhibits as many as 15 oxidation states with an even spacing of electrical potential.[46] Because of fragmentation of clusters and ligand loss in LDI and matrix-assisted laser desorption ionization (MALDI) mass spectrometry analyses, the purity and the exact molecular formula of $Au_{\sim 140}$ species was not attained at that time.[20a] In 2008, Tsukuda et al. developed a method of thermal thiol etching and solvent extraction to obtain core mass of 29 kDa Au clusters and characterized the clusters with electrospray ionization (ESI) mass spectroscopy; the formula of this cluster was, for the first time, determined to be $Au_{144}(SR)_{59}$.[47] It should be noted that our group and Murray group redetermined the formula to be the $Au_{144}(SR)_{60}$ by ESI-MS.[42,48] The one-ligand discrepancy still remains, which is perhaps due to the oxidation pretreatment of the clusters in Tsukuda's work in order to impart charges to the cluster in ESI-

Received: January 16, 2011
Revised: February 25, 2011
Published: March 23, 2011

MS analysis, while in our ESI analysis the cluster ionization was attained by the formation of Cs^+ adducts, the latter method is generally much softer. The theoretical structure of $Au_{144}(SR)_{60}$ has been predicated to be composed of a Au_{114} core and 30 $Au(SR)_2$ staples.[49a] X-ray absorption spectrometry analysis is consistent with the theoretical model.[49b] The exact structure of $Au_{144}(SR)_{60}$ remains to be determined in future work.

To achieve the high purity and high yield of $Au_{144}(SR)_{60}$ clusters, our group previously reported a two-step method to prepare $Au_{144}(SR)_{60}$ using phenylethylthiol.[42] In the first step, a Au cluster mixture with core size near $Au_{\sim 140}$ was synthesized by a modified Brust-Schiffrin method. In the second step, the cluster mixture was converted to truly monodisperse $Au_{144}(SR)_{60}$ clusters by size focusing in the presence of thiols of high concentration and at an elevated temperature (80 °C). This method avoids the complicated size separation process and gives rise to pure $Au_{144}(SR)_{60}$ clusters with relatively high yield (~20%). However, this method still has some limitations. First, an elevated temperature (80 °C) is required for the size focusing process. This process limits the use of low boiling point thiols as the ligands. Second, the intense odor from thiol of high concentration[42] (e.g., 50% PhC_2H_4SH) used for etching Au clusters makes this procedure hard to handle. Thus, we are motivated to develop a facile and straightforward synthetic that involves less stringent experimental conditions and can be easily adapted by researchers in many different fields. This is of particular importance in order to expand the practical applications of this new type of nanomaterial.

In this work, we introduce a simple and robust method to synthesize monodisperse $Au_{144}(SR)_{60}$ clusters at room temperature under ambient conditions. This new method uses only microliters of thiols (hence, much less odored), and is applicable to a range of thiols, including PhC_2H_4SH and various $C_nH_{2n+1}SH$ (n = 4−8). The UV−vis spectra, electrochemistry and powder X-ray diffraction (XRD) of various $Au_{144}(SR)_{60}$ (R = $-C_2H_4Ph$ and $-C_nH_{2n+1}$) are investigated. We have also investigated those potentially important reaction parameters and identified some critical factors for obtaining pure $Au_{144}(SR)_{60}$, including the solvent (methanol), large thiol-to-Au ratios (≥4) and the presence of tetraoctylammonium bromide (TOABr) and O_2 in the reaction system. The ambient synthesis of high-quality $Au_{144}(SR)_{60}$ nanoclusters is of practical importance for achieving a wider range of applications of this new type of material.

EXPERIMENTAL SECTION

Chemicals. All chemicals are commercially available and used as received. Tetraoctylammonium bromide (TOABr, >98%), tetraoctylammonium chloride (TOACl, >98%) and tetrabutylammonium hexafluorophosphate ($TBAPF_6$, 99%) were obtained from Fluka. Tetrachloroauric(III) acid ($HAuCl_4 \cdot 3H_2O$, 99.99%), 2-phenylethanethiol (PhC_2H_4SH, 99%), sodium borohydride ($NaBH_4$, 99.99%), sodium bromide (NaBr, 99.0%), cesium acetate (CsOAc, 99.99%), rubidium acetate (RbOAc, 99.8%), acetone (HPLC grade, 99.9%), methanol (HPLC grade, 99.9%), toluene (HPLC grade, 99.9%) and dichloromethane (HPLC grade, 99.9%) were purchased from Sigma-Aldrich. 1-Butanethiol (C_4H_9SH, 98%), 1-pentanethiol ($C_5H_{11}SH$, 98%), 1-hexanethiol ($C_6H_{13}SH$, 96%), and 1-octanethiol ($C_8H_{17}SH$, 97%) were obtained from Acros Organics.

Synthesis of $Au_{144}(SR)_{60}$ Nanoclusters with PhC_2H_4SH and $C_nH_{2n+1}SH$ (n = 4, 5, 6, 8). All the reactions are conducted at room temperature under air atmosphere. Typically, $HAuCl_4 \cdot 3H_2O$ (0.3 mmol, 118 mg) and TOABr (0.348 mmol, 190 mg) are added to a 50 mL trineck round-bottom flask and mixed with 15 mL of methanol. After being vigorously stirred for 15 min, the solution color changes from yellow to dark red. Then, $C_6H_{13}SH$ or other thiols as mentioned above (1.59 mmol, thiol/Au = 5.3/1) are added to the solution at room temperature; the color of reaction mixture rapidly turns white. After ~15 min, a fresh $NaBH_4$ solution (3 mmol, dissolved in 6 mL of cold Nanopure water) is rapidly added to the solution under vigorous stirring. The color of solution immediately turns black and produces Au clusters, which are then precipitated out of the methanol solution.

The reaction is stopped after ~5 h, and the black precipitates are collected by centrifugation (5 min at ~5000 rpm). The black precipitates are washed with excess methanol and collected by centrifugation again. This step is repeated at least 3 times to completely remove the free thiol residue. Then, CH_2Cl_2 or toluene is used to separate the Au clusters from Au(I)-SR polymers (poorly soluble in almost all solvents). The as-obtained Au clusters only contain $Au_{144}(SR)_{60}$ (major product) and $Au_{25}(SR)_{18}$ (side product see Results and Discussion section). Then, acetone is used to separate the $Au_{144}(SR)_{60}$ and $Au_{25}(SR)_{18}$ clusters. The $Au_{25}(SR)_{18}$ clusters are soluble in acetone, but $Au_{144}(SR)_{60}$ clusters are not, hence, they can be easily separated by centrifugation. The yield of $Au_{144}(SR)_{60}$ clusters is 10−20% (Au atom basis) and the yield of $Au_{25}(SR)_{18}$ cluster is ~5% (Au atom basis); note that the rest of gold is lost to insoluble Au(I)-SR polymers.

Several variations of the above synthetic method are performed to investigate the mechanism of this reaction. In order to study the role of TOABr in the formation of $Au_{144}(SR)_{60}$, we use TOACl and NaBr to replace TOABr. A control experiment (i.e., without TOABr) is also performed. To examine the effect of O_2 in the reaction, the entire reaction is also conducted under a N_2 atmosphere. Various ratios of $C_6H_{13}SH/HAuCl_4$ (4:1, 3:1, and 2:1) are investigated in the experiments.

Characterizations. UV−vis spectra of the Au clusters (dissolved in CH_2Cl_2) were acquired on a Hewlett- Packard (HP) Agilent 8453 diode array spectrophotometer at room temperature. MALDI mass spectrometry was performed with a PerSeptiveBiosystems Voyager DE super-STR time-of-flight (TOF) mass spectrometer using *trans*-2-[3-(4-*tert*-butylphenyl)-2-methyl-2-propenyldidene] malononitrile (DCTB) as matrix.[50] Electrospray ionization (ESI) mass spectra were recorded using a Waters Q-TOF mass spectrometer equipped with a Z-spray source. The source temperature was kept at 70 °C. The sample was directly infused into the chamber at 5 μL/min. The spray voltage was kept at 2.20 kV and the cone voltage at 60 V. The ESI sample was dissolved in toluene (1 mg/mL) and diluted (1:2 v) by dry methanol (containing 50 mM RbOAc or CsOAc to enhance cluster ionization).[42,51] Thermal gravimetric analysis (TGA) (typically ~3 mg sample used) was obtained on a TG/DTA6300 analyzer (Seiko Instruments, Inc.) under a N_2 atmosphere (flow rate ~50 mL/min). The powder X-ray diffraction was conducted on a Panalytical X'Pert Pro MPD X-ray diffractometer. Square wave voltammetry (SWV) and cyclic voltammetry (CV) measurements of Au clusters were performed on a CHI 620C electrochemical station at room temperature under N_2 atmosphere. A platinum wire (counter-electrode), platinum working electrode (2 mm dia.,), and Ag/Ag^+ quasi-reference electrode (QRE) were used in the measurements. Au cluster solution (5−10 mg/mL) was prepared in a $TBAPF_6$ electrolyte solution (0.1 mol/L) in anhydrous CH_2Cl_2, and the solution was first bubbled with dry N_2 to remove O_2 and then blanked under N_2 throughout the electrochemical measurements to minimize O_2 and moisture interference.

RESULTS AND DISCUSSION

1. Size-Focusing Synthesis of $Au_{144}(SC_6H_{13})_{60}$ Clusters in Methanol Phase. The two-phase Brust-Schiffrin method for

Scheme 1. Synthetic Procedure for Monodisperse $Au_{144}(SR)_{60}$ in Methanol (solvent)

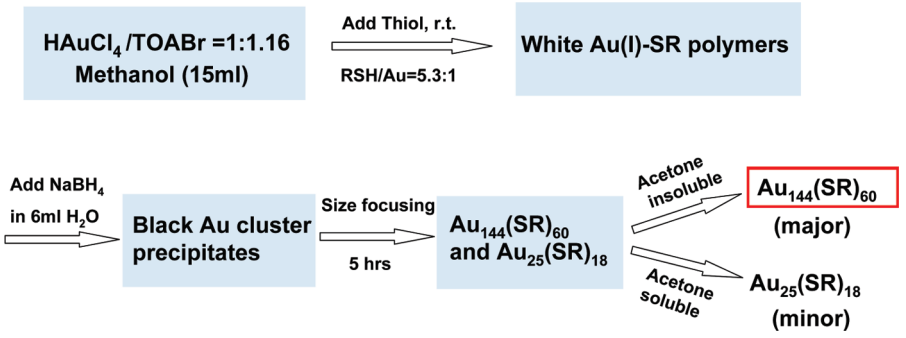

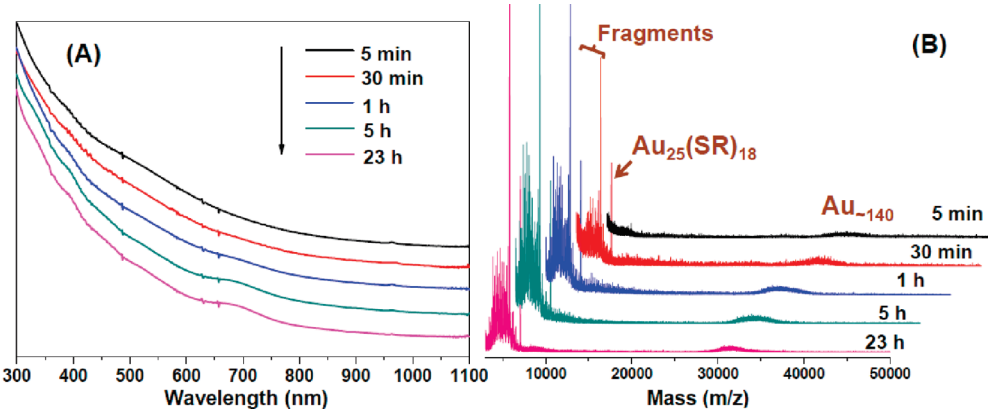

Figure 1. Evolution of (A) UV−vis spectra and (B) MALDI mass spectra of $Au_n(SC_6H_{13})_m$ clusters over the course of size focusing.

preparing thiolate-capped gold nanoparticles involves three steps.[52] First, gold salt precursor (e.g., $HAuCl_4$) is transferred from water phase to toluene phase under the aid of a phase transfer reagent (e.g., TOABr). Then, a specific amount of thiol (RSH) is added, which reduces Au(III) to Au(I)-SR. Finally, the reduction of Au(I)-SR with $NaBH_4$ leads to the formation of Au nanoparticles. In our previous work, we synthesized $[Au_{25}(SR)_{18}]^-$ in high yield and high purity by carefully controlling the reaction kinetics.[53] The atomic monodispersity of the as-obtained clusters led to straightforward crystallization of $[Au_{25}(SR)_{18}]^q$ ($q = -1, 0$) for atomic structure determination by X-ray crystallography.[34,35] However, $Au_{144}(SR)_{60}$ can only be obtained via a two-step, thermal thiol etching method prior to the work presented herein. In this work, a one-pot method has been developed to synthesize monodisperse $Au_{144}(SR)_{60}$ clusters in ambient environment. When methanol is used as the solvent in the reaction, an intriguing size focusing process occurs after the initial formation of Au cluster mixture. The final product only contains $Au_{25}(SR)_{18}$ and $Au_{144}(SR)_{60}$ clusters. Their large solubility difference in acetone renders them easily separable by simple solvent extraction with acetone. Moreover, this procedure is quite versatile for various thiols, including PhC_2H_4SH and $C_nH_{2n+1}SH$ ($n = 4, 5, 6, 8$). This new method is more convenient and easier to handle compared to the previous two-step method.[42] Below, we arbitrarily choose 1-hexanethiol ($C_6H_{13}SH$) as an example for a detailed discussion of the synthesis.

The synthetic procedure is shown in Scheme 1. Details are provided in the Experimental Section. It is worthy of brief discussions about several particular aspects of this procedure. First of all, methanol is used as the solvent for the reaction, which is important to achieve monodisperse $Au_{144}(SR)_{60}$ (main product) and $Au_{25}(SR)_{18}$ (side product). It is because that the Au clusters precipitate from the methanol solvent, which prevents the further growth of Au clusters into larger nanoparticles. The relatively narrow distribution at the initial stage allows the formation of monodisperse clusters after a spontaneous size focusing process. If the synthesis is performed in toluene while keeping other conditions the same, monodisperse $Au_{144}(SR)_{60}$ clusters cannot be obtained. Second, TOABr is intentionally added to the methanol solution of gold precursor ($HAuCl_4$) despite the fact that gold salt is soluble in methanol in the absence of TOABr. The role of TOABr is to be discussed below. Third, a distinctive size focusing phenomenon is observed after the formation of initial size-mixed nanoparticles (denoted as $Au_n(SC_6H_{13})_m$). It is noteworthy that the size focusing phenomenon has also been observed in other syntheses[21,42,47,53,54] and constitutes a universal process in the growth of atomically monodispere $Au_n(SR)_m$ nanoclusters.[55]

The temporal evolution of UV−vis spectra of the $Au_n(SC_6H_{13})_m$ product is shown in Figure 1A, and MALDI mass spectra in Figure 1B. The UV−vis spectra of initial $Au_n(SC_6H_{13})_m$ displays a decaying curve, often indicating a mixture of Au_n clusters. As the reaction continues, a peak at 670 nm as well as some other absorption bands gradually show up, which implies that the size distribution spontaneously narrows down over the reaction process. This size focusing process ends at ~5 h, for that the UV−vis spectra beyond 5 h show no more changes

dx.doi.org/10.1021/cm200143s |Chem. Mater. 2011, 23, 2209–2217

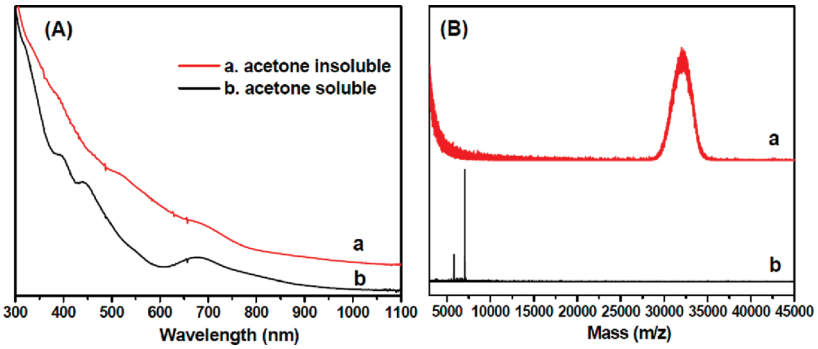

Figure 2. (A) UV−vis spectra and (B) MALDI mass spectra of the acetone soluble and insoluble $Au_n(SC_6H_{13})_m$ clusters.

(Figure 1A). The corresponding MALDI-mass spectra show the conversion of polydisperse Au clusters to $Au_{25}(SR)_{18}$ and $Au_{\sim 140}$ clusters. The initial $Au_n(SC_6H_{13})_m$ clusters (t = 5 min) does not show distinct peaks in the mass spectrum, except for a weak peak at $m/z \approx 31$ k (z = 1), which may be due to the wide size distribution. The weak peak at 31 kDa indicates the existence of $Au_{\sim 140}$ clusters in the initial Au cluster product. After 30 min, a sharp peak at $m/z \approx 7033.9$ and a set of peaks ranging from m/z ~5780.4 to 3500 occur in the low mass range, while the peak at $m/z \approx 31$k become stronger in the high mass range. The peak at $m/z \approx 7033.9$ is easily assigned to $Au_{25}(SC_6H_{13})_{18}$ (calculated FW: 7033.8), and the peak at $m/z \approx 5780.4$ is a fragment ($Au_{21}(SC_6H_{13})_{14}$, calculated FW: 5777.1) of $Au_{25}(SC_6H_{13})_{18}$. The fragmentation pathway of loss of $Au_4(SC_6H_{13})_4$ has been observed in all types of $Au_{25}(SR)_{18}$ with different −R groups.[50,17] As for the set of peaks from m/z 5780 to 3500, they disappear under low laser intensities (see the Supporting Information, Figure S1), indicating that they are also fragments from $Au_{25}(SC_6H_{13})_{18}$; note that, in order to observe the high mass peak at $m/z \approx 31$ k, a relatively higher laser intensity is used, which induces more severe fragmentation of $Au_{25}(SC_6H_{13})_{18}$ clusters.

On the basis of the above MALDI-mass spectral results, the final product (after size focusing) only comprises two species, i.e., $Au_{25}(SC_6H_{13})_{18}$ and $Au_{\sim 140}$ clusters. To isolate them, the reaction was stopped at ~5 h and unreduced Au(I)-SR polymers were removed (see the Experimental Section for details). We found that $Au_{25}(SC_6H_{13})_{18}$ and $Au_{\sim 140}$ clusters can be conveniently separated by acetone. Figure 2 shows the UV−vis spectra and MALDI mass spectra of the acetone soluble and insoluble components. The UV−vis spectrum of the acetone insoluble species (Figure 2A, profile a) exhibits prominent absorption bands at 517 and 700 nm, which matches well with $Au_{144}(SC_2H_4Ph)_{60}$ clusters.[42,47] The corresponding MALDI mass spectrum shows only one peak centered at $m/z \approx 32$ k (note that the peak position slightly shifts with the laser intensity used in MALDI analysis), indicating the high purity of the acetone-isolated Au clusters. The mass peak at $m/z \approx 32$ k (Figure 2B, profile a) is close to the mass of $Au_{144}(SC_6H_{13})_{60}$ (calculated FW: 35 397.0). The deviation of the mass from the calculated value is due to partial loss of $C_6H_{13}S-$ ligands under the MALDI conditions. On the other hand, the UV−vis spectrum of the acetone soluble species (Figure 2A, profile b) shows three distinct peaks at 400, 450, and 670 nm, respectively, which are characteristic of $Au_{25}(SR)_{18}$ clusters.[34] The corresponding MALDI mass spectrum shows two peaks at $m/z \approx 7033.9$ (i.e., $Au_{25}(SC_6H_{13})_{18}$) and 5780.4 (i.e., $Au_{21}(SC_6H_{13})_{14}$, a fragment),

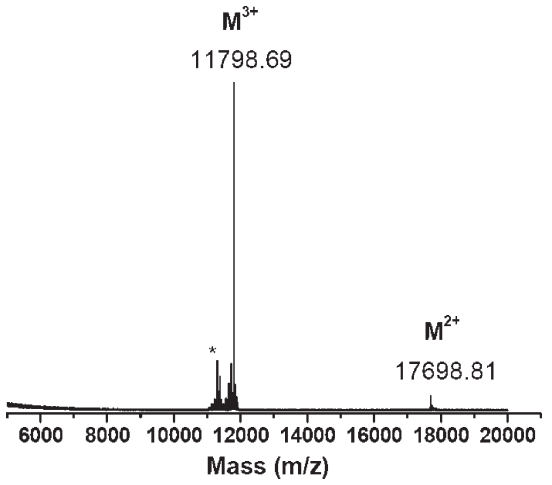

Figure 3. ESI-MS of the acetone-insoluble component identified to be $Au_{144}(SC_6H_{13})_{60}$ clusters. The asterisk shows small fragments of $Au_{144}(SC_6H_{13})_{60}$.

which confirms the composition and purity of the acontone-soluble component. No additional peak at $m/z \approx 32$ k is found in the mass spectrum, demonstrating the complete separation between $Au_{25}(SC_6H_{13})_{18}$ and $Au_{\sim 140}$ clusters with acetone.

MALDI often causes fragmentation of Au clusters and hence complicates the determination of cluster formula. In contrast, ESI is a much softer ionization technique and allows for the observation of the intact molecular ion peak. Herein we employ ESI-MS to determine the composition of the ~32 kDa Au clusters (acetone-insoluble). Two major peaks at $m/z \approx$ 11 798.69 (3+) and 17 698.81 (2+) are observed (Figure 3), which can be easily assigned to triply charged $[Au_{144}(SC_6H_{13})_{60}]^{3+}$ (calculated: 11799.03) and doubly charged $[Au_{144}(SC_6H_{13})_{60}]^{2+}$ (calculated: 17698.55). The zoom-in mass spectra and detailed assignment of all the mass peaks are provided in the Supporting Information, Figure S2 and Table S1. Of note, the small peaks near the main peak ($m/z \approx$ 11798.69) are the fragments from $Au_{144}(SC_6H_{13})_{60}$ after successive loss of two -SC_6H_{13} ligands or a single $Au_4(SC_6H_{13})_4$ unit. The loss of Au_4L_4 seems ubiquitous, which is also observed in $Au_{25}(SR)_{18}$, $Au_{38}(SR)_{24}$, and $Au_{68}(SR)_{34}$ clusters in MALDI-MS analysis.[21a,50,56] Taken together, the high purity of the $Au_{144}(SC_6H_{13})_{60}$ clusters isolated by acetone is confirmed by the ESI-MS analysis because no other Au clusters are found to coexist with $Au_{144}(SC_6H_{13})_{60}$ clusters.

2. Properties of $Au_{144}(SR)_{60}$ Clusters with Various Ligands. The synthetic procedure to prepare $Au_{144}(SR)_{60}$ is quite versatile in terms of the types of thiol ligands. With PhC_2H_4SH and

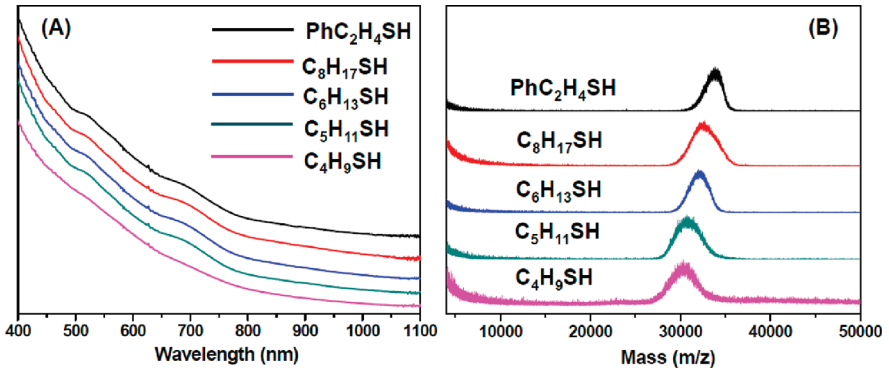

Figure 4. (A) UV−vis spectra and (B) MALDI mass spectra of acetone-insoluble $Au_{144}(SR)_{60}$ clusters. (From top to bottom: RSH = PhC_2H_4SH, $C_8H_{17}SH$, $C_6H_{13}SH$, $C_5H_{11}SH$, and C_4H_9SH).

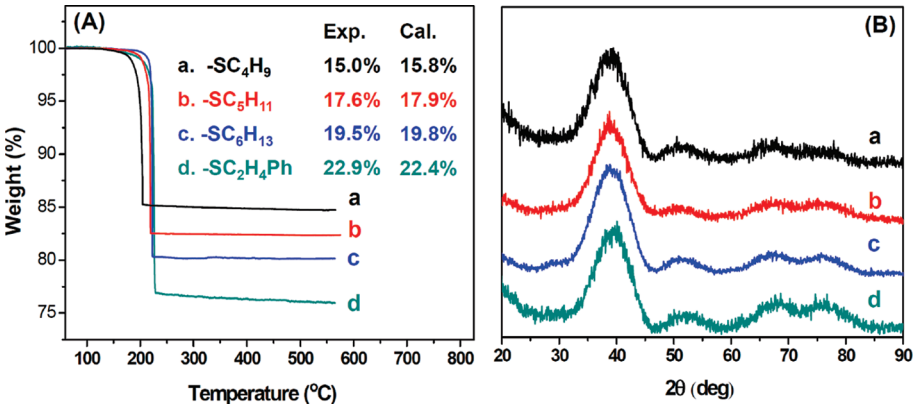

Figure 5. (A) TGA and (B) XRD of Au_{144} clusters with various thiolate ligands (R = $-SC_4H_9$, $-SC_5H_{11}$, $-SC_6H_{13}$, and $-SC_2H_4Ph$). The calculated values of TGA are based on the formula of $Au_{144}(SR)_{60}$.

$C_nH_{2n+1}SH$ (n = 4, 5, 6, 8), following the same synthetic procedure, we have obtained $Au_{144}(SR)_{60}$ clusters. The $Au_{25}(SR)_{18}$ product is similarly isolated by acetone, and the insoluble species is $Au_{144}(SR)_{60}$. Of note, longer chain thiols (n > 12) do not lead to Au_{144} clusters; instead, only Au_{25} clusters in low yield can be obtained.

Figure 4 shows the UV−vis spectra and MALDI mass spectra of Au clusters with PhC_2H_4S-, $C_8H_{17}S$-, $C_6H_{13}S$-, $C_5H_{11}S$- and C_4H_9S- ligands, respectively. All the UV−vis spectra (except the case of butanethiol) display absorption bands at 517 and 700 nm that are characteristic of Au_{144} clusters; thus, these optical absorption bands are not influenced by the type of thiolate ligands. Of note, the absorption peaks of C_4H_9S-protected Au_{144} clusters are not as prominent as other thiolate-protected Au_{144} clusters. We deem that this is due to the existence of some impurity in the acetone-isolated product. In the MALDI spectrum of C_4H_9S-protected Au clusters, a small extra peak at ~23 kDa is observed, apart from the strong peak at ~30 kDa (Figure 4B). This 23 kDa impurity may be responsible for smearing out the absorption bands of $Au_{144}(SC_4H_9)_{60}$. In contrast, PhC_2H_4S-, $C_8H_{17}S$-, $C_6H_{13}S$-, and $C_5H_{11}S$-protected Au_{144} clusters show a single peak at ~33−30 kDa, which indicates the high purity of these Au_{144} clusters (Figure 4B).

Thermogravimetric analysis (TGA) is performed to further confirm the purity and formula of $Au_{144}(SR)_{60}$. The TGA data of the acetone-insoluble $Au_{144}(SR)_{60}$ clusters are shown in Figure 5A. The determined weight loss of $Au_{144}(SR)_{60}$ (R = C_4H_9, C_5H_{11}, C_6H_{13} and C_2H_4Ph) are 15.0, 17.6, 19.5, and 22.9%, respectively, which are consistent with the calculated values (15.8, 17.9, 19.8, and 22.4%) based on the $Au_{144}(SR)_{60}$ formula. From the TGA data, different thiolate protected Au clusters show slightly different thermal stability. The Au clusters protected by thiolate ligands with longer carbon chain show slightly higher stability. For instance, $Au_{144}(SC_4H_9)_{60}$ clusters start to lose organic components at 178 °C, whereas $Au_{144}(SC_5H_{11})_{60}$ and $Au_{144}(SC_6H_{13})_{60}$ clusters start to lose ligands at 195 and 205 °C, respectively. The ESI-MS of C_4H_9S- and $C_8H_{17}S$-protected Au clusters are provided in the Supporting Information, Figure S3, which are unambiguously determined to be $Au_{144}(SC_4H_9)_{60}$ and $Au_{144}(SC_8H_{17})_{60}$.

The powder X-ray diffraction analysis of Au_{144} clusters protected by various thiolate ligands is also performed. The patterns display similar diffraction peaks at 2θ = 39.5, 52, 67, and 77° (Figure 5B), which indicates the core structure of Au_{144} is not affected by the type of thiolate ligand. The $Au_{144}(SR)_{60}$ clusters does not adopt an fcc structure, for that the fcc structure should show peaks at 38, 44, 65, and 77.5°, but the extra peak at 52° rules out the possibility of fcc structure in $Au_{144}(SR)_{60}$ clusters.

We have also investigated the electrochemical properties of the as-prepared $Au_{144}(SR)_{60}$ clusters. Previously, Murray and Quinn and their respective co-workers reported a number of studies of electrochemical behavior of $Au_{\sim 140}$ clusters.[45,46] The $Au_{\sim 140}$ clusters show quantized double layer (QDL) charging

dx.doi.org/10.1021/cm200143s |Chem. Mater. 2011, 23, 2209–2217

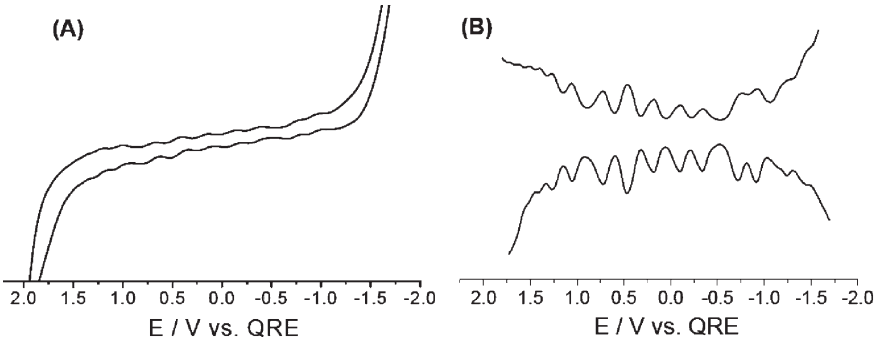

Figure 6. (A) Cyclic voltammetry and (B) square wave voltammetry of $Au_{144}(SC_2H_4Ph)_{60}$ clusters at room temperature.

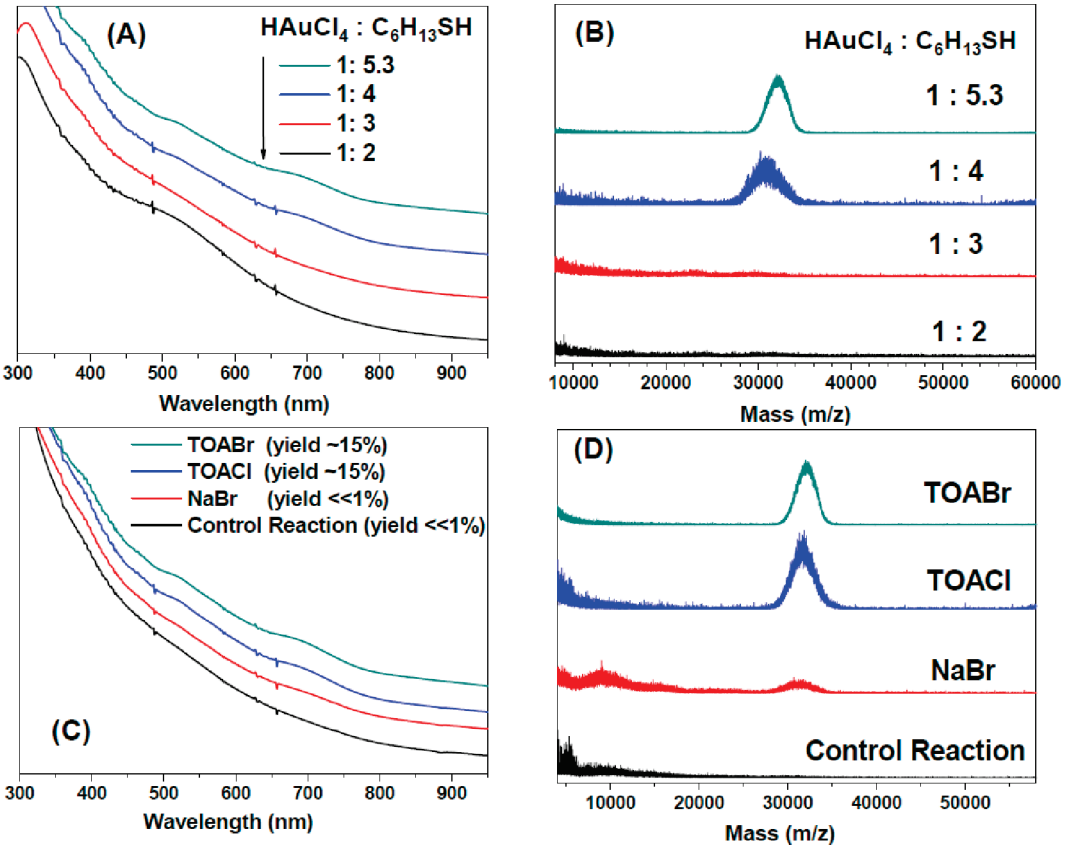

Figure 7. (A) UV−vis spectra and (B) MALDI- mass spectra of $Au_n(SC_6H_{13})_m$ clusters with various $HAuCl_4/C_6H_{13}SH$ ratios (1:5.3, 1:4.0, 1:3.0 and 1:2.0). (C) UV−vis spectra and (D) MALDI-mass spectra of $Au_n(SC_6H_{13})_m$ clusters with TOABr, TOACl, and NaBr, respectively. Note that the control reaction involves no salts.

even at room temperature. The QDL charging of Au clusters occurs because the capacitance of clusters (e.g., sub-aF) is so small that the single electron charging energy ($e^2/2C$) becomes comparable or larger than the thermal energy ($k_BT \approx 0.025$ eV at r.t.). Using $Au_{144}(SC_2H_4Ph)_{60}$ clusters as an example, we performed cyclic voltammetry (CV) and square wave voltammetry (SWV) analyses at room temperature (Figure 6). The $Au_{144}(SC_2H_4Ph)_{60}$ clusters clearly show QDL charging. The SWV of Au clusters (Figure 6B) exhibits 12 distinct current peaks with an almost even peak spacing (ΔV) of ~0.26 V, which is identical to the previously reports.[45] According to the equation ($C_{CLU} = e/\Delta V$),[45] where C_{CLU} is the double layer capacitance, the $Au_{144}(SC_2H_4Ph)_{60}$ capacitance (C_{CLU}) is calculated to be 0.62 aF.

3. Influences of the Gold-to-Thiol ratio, TOABr, and O_2 on the Synthesis. To find out what parameters affect the synthesis of monodisperse $Au_{144}(SR)_{60}$ clusters, we further investigate the influences of the thiol-to-gold ratio, TOABr and O_2 on the synthesis. We choose $C_6H_{13}SH$ as an example for a discussion below.

We first test the influence of gold-to-thiol ratios on the synthesis. Various ratios (1:5.3, 1:4, 1:3, and 1:2) are investigated in the synthesis of Au_{144} clusters (note: the other conditions are kept the same as the typical protocol). As shown in Figure 7A and B, only the gold/thiol ratios of 1:5.3 and 1:4 can lead to $Au_{144}(SR)_{60}$ clusters. As for the gold/thiol ratio of 1:2, the UV−vis spectrum (Figure 7A) starts to exhibit a surface plasmon

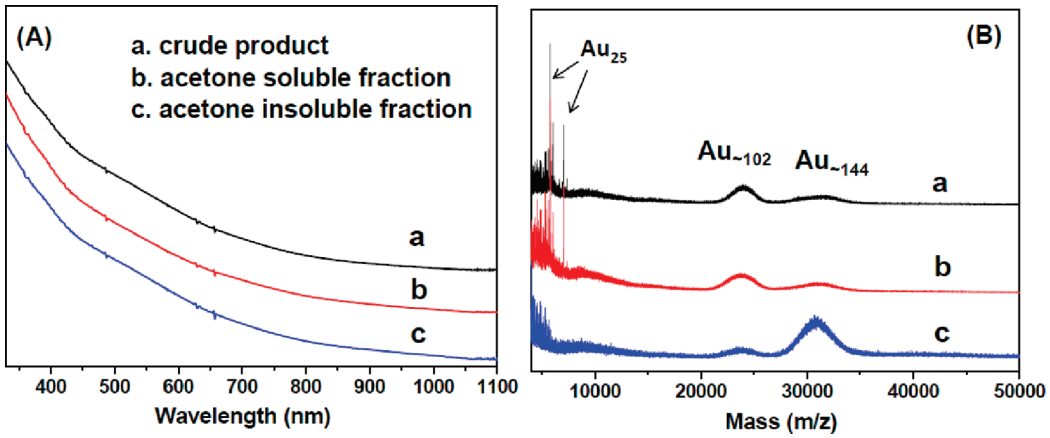

Figure 8. (A) UV−vis spectra and (B) MALDI mass spectra of $Au_n(SC_6H_{13})_m$ clusters made under N_2 atmosphere. (a) Crude product before separation, (b) acetone-soluble fraction, and (c) acetone-insoluble fraction.

band at 520 nm, implying larger (metallic) nanoparticles formed under this condition. Because of the large size of plasmonic Au nanoparticles, no mass peak is observed in the m/z 10 000−60 000 range. For the ratio of 1:3 (often used in previous synthesis of $Au_n(SR)_m$ clusters), the UV−vis spectrum displays a decaying curve without any pronounced peaks, neither does the MALDI mass spectrum show any peaks. These results demonstrate that a large excess of thiol (e.g., thiol/gold >3) is critical for the formation of monodisperse $Au_{144}(SR)_{60}$ clusters. In the size focusing process, excess thiol plays an important role in effecting decomposition of unstable Au_n clusters. Only the stable $Au_{25}(SR)_{18}$ and $Au_{144}(SR)_{60}$ clusters survive the size-focusing process and exist in the final product.

The second important parameter pertains to the role of TOABr in the reaction. In the two-phase synthesis,[52] TOABr serves as the phase transfer agent. Recent reports indicate some effects of TOABr in the formation of small gold nanoparticles.[57] Parker et al. found that TOABr can prevent the oxidation of $[Au_{25}(SR)_{18}]^-$ in the single-phase synthesis (THF as solvent).[18] An interesting question is whether the cation (TOA^+) or the anion (Br^-) plays the role(s). Zhu et al. found that Br^- can indeed effect the conversion of anionic $Au_{25}(SR)_{18}^-$ to neutral $Au_{25}(SR)_{18}^0$ and that TOA^+ can protect $Au_{25}(SR)_{18}^-$ from further attacks by Br^-.[58] The Br^- ions are found to result in decomposition of $Au_{25}(SR)_{18}^-$ clusters as demonstrated in experiments using NaBr (as opposed to TOABr); this is due to the fact that Na^+ does not provide any steric protection for $Au_{25}(SR)_{18}^-$ while TOA^+ does.[58] The important role of Br^- in Au nanorod synthesis has also been identified.[59] Herein, we use TOACl (or NaBr) to replace TOABr in the synthesis. A control reaction without TOABr is also performed. The other conditions are kept the same as the typical protocol involving TOABr. As shown in Figure 7C, D, we obtained $Au_{144}(SR)_{60}$ with similar yield (~15%) in the presence of TOACl; thus, the anion (Cl^- vs Br^-) is not critical in the synthesis, in contrast to the case of Au nanorod synthesis in which Br^- is critical;[59] note that NaI is not tested herein as I^- often results in decomposition of Au clusters,[58] though I^- was previously found to control the seed-mediated growth of anisotropic gold nanoparticles.[60] With respect to the synthesis of Au_{144} clusters, interestingly, we found that the replacement of TOAX (X = Cl or Br) by NaBr leads to only a trace amount of Au_{144} clusters (yield <1%). Furthermore, in the control reaction (i.e., without adding salt of TOAX or NaBr, X = Cl^-, Br^-), no Au_{144} clusters were obtained. These results are somewhat unexpected and clearly indicate that, apart from the excess of thiol (RSH/Au ≥ 4), the TOA^+ ions seems also critical for the formation of $Au_{144}(SR)_{60}$ clusters. We assume that TOA^+ would affect the initial Au(I)-SR polymer structure and renders the polymeric structure suitable for the formation of Au clusters in the step of $NaBH_4$ reduction and subsequent size focusing into Au_{144} clusters; detailed mechanistic studies are still underway.

The third parameter is in regard to the potential influence of O_2 in the synthesis. Previous work has identified the important role of O_2 in Ag nanoprism synthesis[61] and the interactions of O_2 with Au nanoparticles[62] and $Au_{25}(SR)_{18}^-$ clusters.[35,63] Parker et al. found that the presence of oxygen is important for the formation of monodisperse $Au_{25}(SR)_{18}$ in the THF-mediated synthesis.[18] In the Au_{144} synthesis, all the above reactions are conducted in air atmosphere. We speculate that the oxygen in the air may participate in the reaction, particularly in the size focusing process,[55] and thus affect the final products. To examine the effect of O_2 in the reaction, we have conducted the entire reaction under N_2 atmosphere. Figure 8 shows the UV−vis and MALDI mass spectra of $Au_n(SC_6H_{13})_m$ clusters made under a N_2 atmosphere. There is no obvious peak in the UV−vis spectrum of the crude product, nor for the acetone soluble or insoluble fraction, which implies that the product may be a mixture of Au_n clusters. In the corresponding MALDI mass spectra, the crude product and the acetone-soluble fraction contain clusters of $Au_{25}(SC_6H_{13})_{18}$, $Au_{\sim 102}$ ($m/z \approx 24$ k), and less Au_{144} ($m/z \approx 31$ k), whereas the acetone insoluble fraction contains $Au_{\sim 102}$ (less) and predominant Au_{144} clusters. We assign the m/z ~24 k species to $Au_{\sim 102}$ since the calculated mass of "magic size" $Au_{102}(SC_6H_{13})_{44}$ is 25,249; note that the m/z ~1000 deviation should be caused by partial loss of ligands in MALDI analyses, as is observed in $Au_{144}(SR)_{60}$.[42] These results indicate that $Au_{\sim 102}$ survives under the inert atmosphere (without O_2). However, the separation between $Au_{\sim 102}$ and $Au_{\sim 144}$ is very difficult because of their very close size and surface properties. In this work, we focus on the synthesis of monodisperse $Au_{144}(SR)_{60}$ clusters, and therefore, all the reactions are performed under air atmosphere to eliminate $Au_{\sim 102}$ clusters.

■ CONCLUSIONS

In summary, we have developed a facile one-pot method for synthesizing monodisperse $Au_{144}(SR)_{60}$ clusters in an ambient

environment. Furthermore, this synthetic method is demonstrated to be quite versatile for various thiol ligands, including PhC_2H_4SH and $C_nH_{2n+1}SH$ (n = 4−8). The yield of $Au_{144}(SR)_{60}$ is about 10−20%, accompanied by a side-product of $Au_{25}(SR)_{18}$ (~5% yield). The separation of $Au_{144}(SR)_{60}$ from $Au_{25}(SR)_{18}$ is readily achieved by acetone extraction since $Au_{144}(SR)_{60}$ is not soluble in acetone while $Au_{25}(SR)_{18}$ dissolves in acetone. The UV−vis spectra, electrochemical properties and powder XRD analyses of $Au_{144}(SR)_{60}$ with different types of thiol ligands are performed to investigate the optical, electronic and structural properties of $Au_{144}(SR)_{60}$. Furthermore, we identified some critical synthetic conditions for obtaining monodisperse $Au_{144}(SR)_{60}$ clusters in relatively high yield, including the methanol solvent, performing the synthesis under excess thiols (e.g., thiol to Au ratios ≥4), and the presence of O_2 and TOAX (X = Br, Cl). The simple method developed in this work is expect to boost the application studies of $Au_{144}(SR)_{60}$ clusters in many fields, such as catalysis, biomedicine, and optics.

■ ASSOCIATED CONTENT

Supporting Information. MALDI-MS of $Au_n(SC_6H_{14})_m$ clusters in ~5 h with various laser intensity, zoomed-in ESI mass spectra and peaks assignment of acetone-insoluble $Au_n(SC_6H_{13})_m$ clusters, ESI mass spectra of $Au_{144}(SC_4H_9)_{60}$ and $Au_{144}(SC_8H_{17})_{60}$ clusters. This material is available free of charge via the Internet at http://pubs.acs.org.

■ AUTHOR INFORMATION

Corresponding Author
*E-mail: rongchao@andrew.cmu.edu.

■ ACKNOWLEDGMENT

This work is financially supported by CMU, AFOSR, and NIOSH. We thank Dr. Zhongrui Zhou for assistance in ESI-MS analysis.

■ REFERENCES

(1) Rosi, N. L.; Giljohann, D. A.; Thaxton, C. S.; Lytton-Jean, A. K.; Han, M. S.; Mirkin, C. A. *Science* **2006**, *312*, 1027–1030.
(2) Jin, R.; Wu, G.; Li, Z.; Mirkin, C. A.; Schatz, G. C. *J. Am. Chem. Soc.* **2003**, *125*, 1643–1654.
(3) Agasti, S. S.; Chompoosor, A.; You, C.-C.; Ghosh, P.; Kim, C. K.; Rotello, V. M. *J. Am. Chem. Soc.* **2009**, *131*, 5728–5729.
(4) Zhu, Y.; Qian, H.; Drake, B. A.; Jin, R. *Angew. Chem., Int. Ed.* **2010**, *49*, 1295–1298.
(5) Liu, Y.; Tsunoyama, H.; Akita, T.; Tsukuda, T. *Chem. Commun.* **2010**, *46*, 550–552.
(6) Liu, Y.; Tsunoyama, H.; Akita, T.; Xie, S.; Tsukuda, T. *ACS Catal.* **2011**, *1*, 2–6.
(7) (a) Zhu, Y.; Qian, H.; Zhu, M.; Jin, R. *Adv. Mater.* **2010**, *22*, 1915–1920. (b) Zhu, Y.; Wu, Z.; Gayathri, G. C.; Qian, H.; Gil, R. R.; Jin, R. *J. Catal.* **2010**, *271*, 155–160. (c) Zhu, Y.; Qian, H.; Jin, R. *Chem.—Eur. J.* **2010**, *16*, 11455–11462.
(8) (a) Maye, M. M.; Luo, J.; Lin, Y.; Engelhard, M. H.; Hepel, M.; Zhong, C.-J. *Langmuir* **2003**, *19*, 125–131. (b) Maye, M. M.; Lou, Y.; Zhong, C.-J. *Langmuir* **2000**, *16*, 7520–7523.
(9) Garg, N.; Mohanty, A.; Lazarus, N.; Schultz, L.; Rozzi, T. R.; Santhanam, S.; Weiss, L.; Snyder, J. L.; Fedder, G. K.; Jin, R. *Nanotechnology* **2010**, *21*, 405501.
(10) Chen, S. W.; Ingram, R. S.; Hostetler, M. J.; Pietron, J. J.; Murray, R. W.; Schaaff, T. G.; Khoury, J. T.; Alvarez, M. M.; Whetten, R. L. *Science* **1998**, *280*, 2098–2101.
(11) Jin, R. *Nanoscale* **2010**, *2*, 343–362.
(12) Tsunoyama, H.; Nickut, P.; Negishi, Y.; Al-Shamery, K.; Matsumoto, T.; Tsukuda, T. *J. Phys. Chem. C* **2007**, *111*, 4153–4158.
(13) Price, R. C.; Whetten, R. L. *J. Am. Chem. Soc.* **2005**, *127*, 13750–13751.
(14) Varnavski, O.; Ramakrishna, G.; Kim, J.; Lee, D.; Goodson, T., III *ACS Nano* **2010**, *4*, 3406–3412.
(15) Aikens, C. M. *J. Phys. Chem. Lett.* **2011**, *2*, 99–104.
(16) Wyrwas, R. B.; Alvarez, M. M.; Khoury, J. T.; Price, R. C.; Schaaff, T. G.; Whetten, R. L. *Eur. Phys. J. D* **2007**, *43*, 91–95.
(17) (a) Wu, Z.; Gayathri, C.; Gil, R.; Jin, R. *J. Am. Chem. Soc.* **2009**, *131*, 6535–6542. (b) Wu, Z.; Jin, R. *Nano Lett.* **2010**, *10*, 2568–2573.
(18) Parker, J. F.; Weaver, J. E. F.; McCallum, F.; Fields-Zinna, C. A.; Murray, R. W. *Langmuir* **2010**, *26*, 13650–13654.
(19) (a) Watzky, M. A.; Finney, E. E.; Finke, R. G. *J. Am. Chem. Soc.* **2008**, *130*, 11959–11969. (b) Woehrle, G. H.; Hutchison, J. E. *Inorg. Chem.* **2005**, *44*, 6149–6158. (c) Pettibone, J. M.; Hudgens, J. W. *J. Phys. Chem. Lett.* **2010**, *1*, 2536–2540.
(20) (a) Schaaff, T. G.; Shafigullin, M. N.; Khoury, J. T.; Vezmar, I.; Whetten, R. L. *J. Phys. Chem. B* **2001**, *105*, 8785–8796. (b) Kumar, S.; Bolan, M. D.; Bigioni, T. P. *J. Am. Chem. Soc.* **2010**, *132*, 13141–13143. (c) Tang, Z.; Xu, B.; Wu, B.; Germann, M. W.; Wang, G. *J. Am. Chem. Soc.* **2010**, *132*, 3367–3374.
(21) (a) Qian, H.; Zhu, Y.; Jin, R. *ACS Nano* **2009**, *3*, 3795–3803. (b) MacDonald, M.; Zhang, P.; Chen, N.; Qian, H.; Jin, R. *J. Phys. Chem. C* **2010**, *115*, 65–69.
(22) (a) Negishi, Y.; Nobusada, K.; Tsukuda, T. *J. Am. Chem. Soc.* **2005**, *127*, 5261–5270. (b) Ikeda, K.; Kobayashi, Y.; Negishi, Y.; Seto, M.; Iwasa, T.; Nobusada, K.; Tsukuda, T.; Kojima, N. *J. Am. Chem. Soc.* **2007**, *129*, 7230–7231. (c) Tsunoyama, R.; Tsunoyama, H.; Pannopard, P.; Limtrakul, J.; Tsukuda, T. *J. Phys. Chem. C* **2010**, *114*, 16004–16009.
(23) Femoni, C.; Iapalucci, M. C.; Longoni, G.; Zacchini, S.; Zarra, S. *J. Am. Chem. Soc.* **2011**, *133*, 2406–2409.
(24) Tran, N. T.; Powell, D. R.; Dahl, L. F. *Angew. Chem., Int. Ed.* **2000**, *39*, 4121–4125.
(25) (a) Habeeb Muhammed, M. A.; Pradeep, T. *Small* **2011**, *7*, 204–208. (b) Shibu, E. S.; Muhammed, M. A. H.; Tsukuda, T.; Pradeep, T. *J. Phys. Chem. C* **2008**, *112*, 12168–12176.
(26) Harkness, K. M.; Fenn, L. S.; Cliffel, D. E.; McLean, J. A. *Anal. Chem.* **2010**, *82*, 3061–3066.
(27) (a) Knoppe, S.; Dharmaratne, A. C.; Schreiner, E.; Dass, A.; Burgi, T. *J. Am. Chem. Soc.* **2010**, *132*, 16783–16789. (b) Yao, H.; Fukui, T.; Kimura, K. *J. Phys. Chem. C* **2007**, *111*, 14968–14976.
(28) Toikkanen, O.; Ruiz, V.; Ronholm, G.; Kalkkinen, N.; Liljeroth, P.; Quinn, B. M. *J. Am. Chem. Soc.* **2008**, *130*, 11049–11055.
(29) (a) Qian, H.; Zhu, Y.; Jin, R. *J. Am. Chem. Soc.* **2010**, *132*, 4583–4585. (b) Zhu, M.; Qian, H.; Jin, R. *J. Am. Chem. Soc.* **2009**, *131*, 7220–7021. (c) Zhu, M.; Qian, H.; Jin, R. *J. Phys. Chem. Lett.* **2010**, *1*, 1003–1007.
(30) Negishi, Y.; Kurashige, W.; Niihori, Y.; Iwasa, T.; Nobusada, K. *Phys. Chem. Chem. Phys.* **2010**, *12*, 6219–6225.
(31) Sakai, N.; Tatsuma, T. *Adv. Mater.* **2010**, *22*, 3185–3188.
(32) Jadzinsky, P. D.; Calero, G.; Ackerson, C. J.; Bushnell, D. A.; Kornberg, R. D. *Science* **2007**, *318*, 430–433.
(33) Heaven, M. W.; Dass, A.; White, P. S.; Holt, K. M.; Murray, R. W. *J. Am. Chem. Soc.* **2008**, *130*, 3754–3755.
(34) Zhu, M.; Aikens, C. M.; Hollander, F. J.; Schatz, G. C.; Jin, R. *J. Am. Chem. Soc.* **2008**, *130*, 5883–5885.
(35) Zhu, M.; Eckenhoff, W. T.; Pintauer, T.; Jin, R. *J. Phys. Chem. C* **2008**, *112*, 14221–14224.
(36) Qian, H.; Eckenhoff, W. T.; Zhu, Y.; Pintauer, T.; Jin, R. *J. Am. Chem. Soc.* **2010**, *132*, 8280–8281.
(37) Walter, M.; Akola, J.; Lopez-Acevedo, O.; Jadzinsky, P. D.; Calero, G.; Ackerson, C. J.; Whetten, R. L.; Gronbeck, H.; Hakkinen, H. *Proc. Natl. Acad. Sci. U.S.A.* **2008**, *105*, 9157–9162.

(38) Jiang, D.; Tiago, M. L.; Luo, W.; Dai, S. *J. Am. Chem. Soc.* **2008**, *130*, 2777–2779.
(39) Gao, Y.; Shao, N.; Zeng, X. C. *ACS Nano* **2008**, *2*, 1497–1503.
(40) Zhu, M.; Aikens, C. M.; Hendrich, M. P.; Gupta, R.; Qian, H.; Schatz, G. C.; Jin, R. *J. Am. Chem. Soc.* **2009**, *131*, 2490–2492.
(41) Whetten, R. L.; Price, R. C. *Science* **2007**, *318*, 407–408.
(42) Qian, H.; Jin, R. *Nano Lett.* **2009**, *9*, 4083–4087.
(43) Whetten, R. L.; Khoury, J. T.; Alvarez, M. M.; Murthy, S.; Vezmar, I.; Wang, Z. L.; Stephens, P. W.; Cleveland, C. L.; Luedtke, W. D.; Landman, U. *Adv. Mater.* **1996**, *8*, 428–433.
(44) Ingram, R. S.; Hostetler, M. J.; Murray, R. W.; Schaaff, T. G.; Khoury, J. T.; Whetten, R. L.; Bigioni, T. P.; Guthrie, D. K.; First, P. N. *J. Am. Chem. Soc.* **1997**, *119*, 9279–9280.
(45) Hicks, J. F.; Miles, D. T.; Murray, R. W. *J. Am. Chem. Soc.* **2002**, *124*, 13322–13328.
(46) Quinn, B. M.; Liljeroth, P.; Ruiz, V.; Laaksonen, T.; Kontturi, K. *J. Am. Chem. Soc.* **2003**, *125*, 6644–6645.
(47) Chaki, N. K.; Negishi, Y.; Tsunoyama, H.; Shichibu, Y.; Tsukuda, T. *J. Am. Chem. Soc.* **2008**, *130*, 8608–8610.
(48) Fields-Zinna, C. A.; Sardar, R.; Beasley, C. A.; Murray, R. W. *J. Am. Chem. Soc.* **2009**, *131*, 16266–16271.
(49) (a) Lopez-Acevedo, O.; Akola, J.; Whetten, R. L.; Gronbeck, H.; Hakkinen, H. *J. Phys. Chem. C* **2009**, *113*, 5035–5038. (b) MacDonald, M. A.; Zhang, P.; Qian, H.; Jin, R. *J. Phys. Chem. Lett.* **2010**, *1*, 1821–1825.
(50) Dass, A.; Stevenson, A.; Dubay, G. R.; Tracy, J. B.; Murray, R. W. *J. Am. Chem. Soc.* **2008**, *130*, 5940–5946.
(51) Tracy, J. B.; Crowe, M. C.; Parker, J. F.; Hampe, O.; Fields-Zinna, C. A.; Dass, A.; Murray, R. W. *J. Am. Chem. Soc.* **2007**, *129*, 16209–16215.
(52) Brust, M.; Walker, M.; Bethell, D.; Schiffrin, D. J.; Whyman, R. *Chem. Commun.* **1994**, 801–802.
(53) (a) Zhu, M.; Lanni, E.; Garg, N.; Bier, M. E.; Jin, R. *J. Am. Chem. Soc.* **2008**, *130*, 1138–1139. (b) Wu, Z.; Suhan, J.; Jin, R. *J. Mater. Chem.* **2009**, *19*, 622–626.
(54) Dharmaratne, A. C.; Krick, T.; Dass, A. *J. Am. Chem. Soc.* **2009**, *131*, 13604–13605.
(55) Jin, R.; Qian, H.; Wu, Z.; Zhu, Y.; Zhu, M.; Mohanty, A.; Garg, N. *J. Phys. Chem. Lett.* **2010**, *1*, 2903–2910.
(56) Dass, A. *J. Am. Chem. Soc.* **2009**, *131*, 11666–11667.
(57) Goulet, P. J. G.; Lennox, R. B. *J. Am. Chem. Soc.* **2010**, *132*, 9582–9584.
(58) Zhu, M.; Chan, G.; Qian, H.; Jin, R. *Nanoscale* **2010**, DOI: 10.1039/C0NR00878H.
(59) Garg, N.; Scholl, C.; Mohanty, A.; Jin, R. *Langmuir* **2010**, *26*, 10271–10276.
(60) Millstone, J. E.; Wei, W.; Jones, M. R.; Yoo, H.; Mirkin, C. A. *Nano Lett.* **2008**, *8*, 2526–2529.
(61) Xue, C.; Metraux, G. S.; Millstone, J. E.; Mirkin, C. A. *J. Am. Chem. Soc.* **2008**, *130*, 8337–8344.
(62) Dasog, M.; Scott, R. W. J. *Langmuir* **2007**, *23*, 3381–3387.
(63) Shichibu, Y.; Negishi, Y.; Tsukuda, T.; Teranishi, T. *J. Am. Chem. Soc.* **2005**, *127*, 13464–13465.